

AD-A201 983

3

OFFICE OF NAVAL RESEARCH

Contract N00014-80-K-0852

R&T Code _____

Technical Report No. 48

Chemical Effects in the Carbon KVV Auger Lineshapes

By

D. E. Ramaker

Prepared for Publication

in the

Journal Of Vacuum Science and Technology

George Washington University
Department of Chemistry
Washington, D.C. 20052

December, 1987

Reproduction in whole or in part is permitted for
any purpose of the United States Government

This document has been approved for public release
and sale; its distribution is unlimited.

DTIC
ELECTE
DEC 19 1988
S H D

SECURITY CLASSIFICATION OF THIS PAGE

REPORT DOCUMENTATION PAGE

1a. REPORT SECURITY CLASSIFICATION Unclassified			1b. RESTRICTIVE MARKINGS		
2a. SECURITY CLASSIFICATION AUTHORITY			3. DISTRIBUTION / AVAILABILITY OF REPORT Approved for Public Release, distribution Unlimited.		
2b. DECLASSIFICATION / DOWNGRADING SCHEDULE					
4. PERFORMING ORGANIZATION REPORT NUMBER(S) Technical Report # 48			5. MONITORING ORGANIZATION REPORT NUMBER(S)		
6a. NAME OF PERFORMING ORGANIZATION Dept. of Chemistry George Washington Univ.		6b. OFFICE SYMBOL (If applicable)	7a. NAME OF MONITORING ORGANIZATION Office of Naval Research (Code 413)		
6c. ADDRESS (City, State, and ZIP Code) Washington, D.C. 20052			7b. ADDRESS (City, State, and ZIP Code) Chemistry Program 800 N. Quincy Street Arlington, VA 22217		
8a. NAME OF FUNDING / SPONSORING ORGANIZATION Office of Naval Research		8b. OFFICE SYMBOL (If applicable)	9. PROCUREMENT INSTRUMENT IDENTIFICATION NUMBER Contract N00014-80-K-0852		
8c. ADDRESS (City, State, and ZIP Code) Chemistry Program 800 North QUINCY, Arlington, VA 22217			10. SOURCE OF FUNDING NUMBERS		
			PROGRAM ELEMENT NO. 61153 N	PROJECT NO.	TASK NO. PP 013-08-01
			WORK UNIT ACCESSION NO. NR 056-681		
11. TITLE (Include Security Classification) Chemical Effects in the Carbon KVV Auger Lineshapes (Uncl.)					
12. PERSONAL AUTHOR(S) D. E. Ramaker					
13a. TYPE OF REPORT		13b. TIME COVERED FROM TO		14. DATE OF REPORT (Year, Month, Day)	
				15. PAGE COUNT 17	
16. SUPPLEMENTARY NOTATION Prepared for Publication in Journal of Vacuum Science and Technology					
17. COSATI CODES			18. SUBJECT TERMS (Continue on reverse if necessary and identify by block number)		
FIELD	GROUP	SUB-GROUP	Auger Spectroscopy, Hydrocarbons, Polyethylene, Electron Correlation. (ALW)		
19. ABSTRACT (Continue on reverse if necessary and identify by block number)					
<p>We review the results of a consistent quantitative interpretation of the KVV Auger line shapes of five different gas phase hydrocarbons (methane, ethane, cyclohexane, benzene, and ethylene), three solids (polyethylene, diamond, and graphite), and a molecularly chemisorbed system (ethylene/di). The normal kvv line shape accounts for only about half of the total experimental intensity for most of the Auger line shapes. The remaining part of the experimental line shape can be attributed to satellites resulting from resonant excitation or dynamic screening processes. The normal kvv Auger lines shapes are seen to reflect delocalized holes, however correlation effects are very evident. Although these screening and correlation effects complicate the interpretation of the line shapes, they provide a means to obtain unique chemical, electronic, and bonding information, and indeed cause the principal differences seen among the experimental line shapes. <u>Keywords:</u></p>					
20. DISTRIBUTION / AVAILABILITY OF ABSTRACT <input checked="" type="checkbox"/> UNCLASSIFIED/UNLIMITED <input checked="" type="checkbox"/> SAME AS RPT. <input type="checkbox"/> OTC USERS			21. ABSTRACT SECURITY CLASSIFICATION Unclassified		
22a. NAME OF RESPONSIBLE INDIVIDUAL Dr. David L. Nelson			22b. TELEPHONE (Include Area Code) (202) 696-4410		22c. OFFICE SYMBOL

DD FORM 1473, 84-MAR

83 APR edition may be used until exhausted.
All other editions are obsolete.SECURITY CLASSIFICATION OF THIS PAGE
Unclassified

88 12 12 168

1. Introduction

Auger electron spectroscopy (AES) is often capable of yielding information concerning the chemical environment of atoms in gas phase molecules or in the near-surface region of a solid. This information is manifested as "changes in the observed AES for a particular element in the specimen under study, compared to a spectrum produced by the same element when it is in some reference form" [1]. These chemical effects may result in 1) a shift in the energy of an Auger peak, 2) a change in the shape of an Auger electron energy distribution often called the line shape, or 3) a change in the Auger signal strengths of an Auger transition. In this work we limit our consideration to changes in the Auger line shape. An understanding of the Auger line shape changes requires a thorough understanding of the factors contributing to the Auger process. This is a formidable task, but it provides the greatest potential payoff; namely detailed information on the bonding and electronic structure of the atom in question, and even information concerning the movement of electronic charge upon creation of a core or valence hole.

To obtain chemical or electronic structure information from AES requires two major efforts; first one must extract a true Auger line shape from the raw Auger spectrum, and second, one must derive a theoretical framework for semi-quantitative interpretation of that line shape. We and others have previously summarized current methods for extracting the line shape [2,3] and presented a theoretical framework for the line shape interpretation [4]. In this work we review recent applications involving the carbon atom in its varied allotropic and chemical forms.

The nature of this article is not to review the extensive literature on AES; a large number of review articles has appeared in the last five years [4,5]. Rather this article summarizes our recent work on the C KVV Auger line



Dist		Avail and/or Special	
A-1			

ides

shapes in several gas phase hydrocarbons (methane, ethane, ethylene, benzene, and cyclohexane) [6], solids (graphite, diamond, polyethylene) [7-9] and chemisorbed systems (molecular and fragmented ethylene on Ni(100)) [10]. It examines the dramatic effects of final state hole-hole correlation and core-hole screening, how they change from the gas phase molecular, condensed molecular, and solid states, and how these can be used to learn something about the chemical and electronic properties of the material under study.

2. Overview

In many respects, this work can be viewed as a sequel to the reviews we published previously [4,11]. Therefore we will present only a summary of the theoretical framework. Before doing so we present an overview (Fig. 1) of the experimental Auger line shapes [7, 12-14] and compare them with the self-fold of the appropriate one-electron density of states (DOS),

$$\rho^2\rho(E) = \int \rho(E-\epsilon)\rho(\epsilon)d\epsilon, \quad (1)$$

which is known to represent a first approximation to the line shape. The empirical procedure for obtaining the DOS has been described previously [6-10]. It involves the use of x-ray emission (XES) and photoelectron (XPS) spectra, and in some cases theoretical calculations. For two reasons, we utilize semi-empirically derived DOS, even for simple molecules. First, most one-electron theoretical calculations do not include electron correlation effects and therefore do not give sufficiently accurate binding energies. Second, the semi-empirical DOS include approximate widths for each orbital feature.

Assuming the XES and XPS spectra utilized to obtain the DOS were measured at sufficiently high resolution, these widths primarily reflect broadening due to the vibrational state manifold of the final state which project onto the core initial state in XES, or ground state in PES. $\rho^2\rho(E)$ then has twice the broadening consistent with the Auger two-hole final state. The Auger line shapes in Fig. 1 for the gas phase hydrocarbons are the raw data, those for

the solids are obtained from the data after background subtraction and deconvolution utilizing well-known procedures [2,3].

Fig. 1 reveals several important points. First, note that the experimental line shape for the gas phase molecules is shifted by about 6-10 eV to higher two-electron binding energy (or lower Auger kinetic energy). The binding energy scale is determined by subtracting the Auger kinetic energy from the C K binding energy [i.e. $E_b = -(E_k - K_{Mg})$]. This shift of the experimental line shape to higher binding energy is due to final state hole-hole repulsion, since the two holes cannot completely delocalize. No shift is seen for the solids, since in this case the holes can completely delocalize. However, hole-hole correlation effects are seen in all of the experimental line shapes, as indicated by the clear distortions from the one-electron self-fold. The second interesting point concerns the onset or threshold of the spectra. Although the principal peaks of the gas phase experimental spectra are shifted to higher binding energy, the onsets of both the experimental line shape and the DOS self-fold for each case are essentially the same. This suggests that each of the spectra has at least some contribution which arises from a process producing a final state with a smaller hole-hole repulsion. Furthermore, note that each experimental spectrum extends to much higher binding energy than does the DOS self-fold, indicating a process producing a final state with a higher hole-hole repulsion. We will show that the processes producing these satellite contributions are resonant excitation and initial-state and final-state shakeoff.

We shall refer to these satellites as the $ke-vve$, $ke-v kv-vvv$ and $k-vvv$ satellites, where the notation indicates the particles in the initial and final state before and after the hyphen. Here, the "k" refers to the initial 1s core hole, the "e" to the resonantly excited bound electron, and v to a valence hole created either by the shakeoff process or by the Auger decay. The principal

Auger process is indicated without the hyphen (kvv rather than k-vv) consistent with that used historically. We use kvv to indicate this principal or normal Auger contribution to differentiate it from the total KVV experimental line shape.

In light of the above, the line shape consists of the sum of several contributions ; namely,

$$N(E) = c_1 I_{kvv}(E) + c_2 I_{ke-vve}(E) + c_3 I_{ke-v}(E) + c_4 I_{kv-vvv}(E) + c_5 I_{k-vvv}(E). \quad (2)$$

The process creating each component is illustrated in Fig. 2. Here the ke-vve term refers to the resonant Auger satellite, which arises when Auger decay occurs in the presence of a localized electron, which was created by resonant excitation into an excitonic or bound state upon creation of the core hole. The ke-v contribution arises when the resonantly excited electron participates in the Auger decay. The kv-vvv term is the initial-state shake Auger term arising when Auger decay occurs in the presence of a localized valence hole, which was created via the shakeoff process during the initial ionization. The k-vvv term denotes the final state shake Auger satellite, which arises when Auger decay occurs simultaneously with shakeoff of a valence hole. These latter two terms arise as a direct result of core hole screening. The ke-vve and ke-v terms arise because the Auger process is generally excited by electron excitation which allows the resonant excitation. The coefficients in eq. 2 are obtained by least squares fit to the experimental spectra.

3. Theoretical framework

3.1 The principal kvv line shape

Our theoretical prescription [6] for generating the kvv term can best be expressed by the eq.

$$I_{kvv}(E) = B \sum_n [P_{kn} R_n R_p A(E + \delta_{11}, \Delta U_{11}, \rho_1, \rho_p)]. \quad (3)$$

The Cini function [15],

$$A(E, \Delta U, \rho, \rho') = \frac{\rho^* \rho'(E)}{[1 - \Delta U I(E)]^2 + [\Delta U \pi \rho^* \rho'(E)]^2}, \quad (4)$$

introduces hole-hole correlation effects. Here ΔU is the effective hole-hole correlation parameter and $I(E)$ is the Hilbert transform,

$$I(E) = \int \rho(\epsilon)/(E - \epsilon) d\epsilon. \quad (5)$$

The Cini function, which distorts the DOS self-fold for treatment of Auger line shapes in solids, mimics the effects of configuration interaction theory on the DOS for molecules [6,16]. Thus it can be used (albeit with some modifications) on the DOS self-fold for molecules as well. In eq.(3) we have included additional arguments in A to make explicit the point that the total theoretical kvv line shape is a sum of components, with each ll' component having an energy shift, $\delta_{ll'}$, and a hole-hole correlation parameter, $\Delta U_{ll'}$, and with each component derived from a fold of the ρ_l and $\rho_{l'}$ DOS as defined in eq. (1). The subscripts λ are defined below. The atomic Auger matrix elements $P_{kl\lambda}$ (normalized per electron) are obtained from experimental and theoretical results for neon [4,11]. The relative magnitudes utilized in this work are $P_{kss} = 0.8$, $P_{ksp} = 0.5$, and $P_{kpp} = 1$, as reported previously [4]. In eq.(3), B is a normalization constant and the R_i are core hole screening factors defined as below.

We have shown previously [16,17] that in covalent systems, intermediate levels of localization can occur. As ΔU increases relative to the effective covalent interaction, the holes localize first from the bond or molecular orbital to a "cluster" orbital, and then to a bond orbital. A simple examination of the MO's for the alkanes or diamond [18] suggests strongly that the appropriate local orbital for these carbon based systems is the tetrahedral cluster orbital involving four sp^3 bond orbitals surrounding a single C atom. Similarly, for the alkenes or graphite, the appropriate local orbital is the sp^2 cluster for the σ bonds, and a single p orbital for the π bonds [18]. In light of the

above, the ΔU 's can be interpreted in this work as the difference between the hole-hole repulsion when two holes are localized on the same local cluster orbital (U_{11}) verses when they are localized on different neighboring cluster orbitals (U_{12}). The δ parameters can be interpreted as the repulsion energy when the holes are completely delocalized about the system [6]. They remain finite for molecules, and are zero for the extended covalent solids.

The subscripts $\lambda\lambda'$ in eq. (3) on the ΔU and δ parameters are to make explicit that these parameters vary with the nature of the orbital combination. Thus for the alkanes we allow three different ΔU 's, namely for the CH-CH, CH-CC, and CC-CC σ orbital combinations, and for the alkenes three different ΔU 's, namely for the $\sigma\sigma$, $\sigma\pi$, and $\pi\pi$ orbital combinations. With this prescription, the separate ss, sp, and pp angular momentum contributions to the Auger line shape, which belong to the same $\lambda\lambda'$ contribution, are required to have the same ΔU and δ parameters. There are generally six different Π' contributions, but we allow only three different ΔU and δ parameters for each molecule, and these are determined to provide optimal agreement with experiment [6-10].

The factors R_i in eq. (3) are to make our theory consistent with the previously derived final state rule for Auger line shapes [19]. The final state rule indicates that 1) the shape of the individual Π' contributions should reflect the DOS in the final state, and 2) the intensity of each Π' contribution should reflect the electron configuration of the initial state. For the kvv line shape, the final state is without the core hole. We assume that the DOS in the final state and ground state are similar, so the spectral shape of ρ_i should reflect the ground DOS. However, the initial state in the kvv process has a core hole, therefore the integrated ρ_i should reflect the electron configuration of the initial core hole (CHS) state. The R_i factors are defined,

$$R_i = \int \rho_{CHS,i}(c) dc / \int \rho_i(c) dc. \quad (6)$$

In this work we assume all R_i are similar so that they can be ignored. Effectively this ignores the "static" effects of core hole screening; the shakeoff contributions are "dynamic" core hole screening effects which are included.

3.2 The satellites

The ke-vve and kv-vvv satellites are also generated by eq. 3 but with different values for ΔU_{ii} and δ_{ii} [6]. For the ke-vve satellite the spectator electron can screen the two holes and reduce the repulsion. We assume that ΔU_{ii} is zero (i.e. no distortion due to correlation occurs), and determine δ_{ii} empirically for optimum fit to experiment. Of course δ_{ii} should be smaller than for the kvv case. For the kv-vvv satellite, the three hole final state experiences a larger effective repulsion. We have shown previously [6,9] that it is twice that for the kvv term if the shake hole is localized on the methyl group or atom with the core hole, and equal to that for kvv if it is delocalized throughout some larger subcluster of the molecule. Of course in the solid, no kv-vvv satellite appears if the shake hole completely delocalizes. δ_{kv-vvv} is again determined empirically and should be larger than for δ_{kvv} .

The ke-v satellite can be generated from eq. 3 assuming that the sum over l' is limited to the orbital with the resonantly excited electron [6]. Again ΔU is zero, since a single hole exists in the final state, and δ_{ii} , determined empirically, is equal to the exciton binding energy. The k-vvv satellite is generated by the Bethe expression, $\log(E/E_{th})/(E/E_{th})^m$ for $E > E_{th}$ [2,6]. E_{th} is a parameter representative of the threshold energy for intrinsic loss, and m is a parameter usually around one [2].

The basic processes for C_2H_4/Ni are different from that for the others, but they can be related to the gas phase molecular case (e.g. ethylene) [10]. The spectrum in Fig. 3b was excited by x-rays, so that no resonant satellites should appear [20]. However, charge transfer from the substrate into the π^*

orbital occurs to screen the holes, in both the core-hole initial state and the two- or three-hole Auger final state. This charge transfer has the affect of decreasing the ΔU and δ parameters; the transferred charge playing the role of the resonantly excited electron in the gas phase [10]. Thus the kvv and $kv-vvv$ contributions which comprise the intramolecular component (i.e. termed the VV component in ref 10) for the chemisorbed state are similar to the $ke-vve$ and kvv in the gas. The $V\pi^*$ component is similar to the $ke-v$, and the $\pi^*\pi^*$ component is a new contribution unlike that of any in the gas phase, in fact it is approximated in Fig 3b by the Ni $L_{2,3}VV$ Auger line shape [10].

Although the latter two components are facilitated through an intra-atomic $V\pi^*$ and $\pi^*\pi^*$ Auger process, respectively, they ultimately appear inter-atomic in character because one or both holes ultimately end up on the substrate.

4. Application to the C KVV line shapes

Figs. 3-6 compare the optimal theoretical line shape and each of the components with the experimental line shapes for ethylene [21], ethylene/Ni [20], benzene [13], polyethylene [12,23], and diamond [13,22]. In general the theoretical line shapes generated by the prescription above agrees nicely with the experimental line shapes. Similarly good agreement is obtained for the systems not shown, i.e. for methane, ethane, cyclohexane, and graphite. Table 1 summarizes the ΔU and δ parameters for the principal kvv components, and Table 2 the results for the satellites.

4.1 The kvv component

Table 1 reveals that for the alkanes the ΔU 's are larger for the CH MO's than for the CC MO's. This can be understood simply from the more localized character of a CH orbital about a single C atom (increased U_{11}), and decreased interaction between CH cluster orbitals (decreased U_{12}), compared with CC cluster orbitals [18]. Likewise for the alkenes, contributions involving only the π MO's have a zero ΔU . This is consistent with one's chemical intuition

concerning the de-localized π orbitals and also consistent with that found previously for graphite. Generally within a single molecule the ΔU 's decrease in the order $\sigma\sigma > \sigma\pi > \pi\pi$ for the alkenes, and $\text{CH-CH} > \text{CH-CC} > \text{CC-CC}$ for the alkanes as expected.

Note that the ΔU 's for the CH-CH orbital in methane and for the CC-CC orbital in ethane are zero. This is by design [6]. Since only one of these cluster orbitals exist for each molecule, no CI distortion effects (at least of the type included by the Cini expression) are expected for these contributions. Since at least two CH orbitals exist in ethane, the CH-CH and CH-CC contributions have non-zero ΔU 's.

Multiplet effects are becoming large in the smaller molecules, such as methane, ethane and ethylene. This is particularly evident in the ethylene spectrum. The two peaks between 30 and 40 eV in the theoretical kVV line shape have widely different intensity, however in the experimental spectrum they have similar intensity (see Fig. 3). We have shown previously [6] that this arises because of multiplet splitting which is absent in our theory.

Comparison of the ΔU 's between molecules indicates something about the nature of the screening processes in these molecules. Note that the ΔU for the CC-CC contribution increases in the order cyclohexane < polyethylene < diamond. This can be understood from the definition of $\Delta U = U_{11} - U_{12}$. For very short screening lengths, one might expect both U_{11} and U_{12} to be reduced substantially, so that ΔU would be decreased [7]. For long screening lengths, one might expect U_{12} to be decreased more than U_{11} , having the effect of increasing ΔU . We believe that the latter is occurring in the current systems. The longer chain length in polyethylene and full three dimensional covalency in diamond suggests that the extent of polarization should increase in the order cyclohexane < polyethylene < diamond. This increased polarization then has the effect of increasing ΔU . For the alkenes, the ΔU 's

are all the same. This suggests that the screening length is much shorter so that "full" screening already occurs in ethylene. This is consistent with the more delocalized π electrons in the alkenes.

The variation of the δ parameter is not as systematic as that found for ΔU ; nevertheless, some important trends are evident. We can interpret the δ 's as the delocalized molecular hole-hole repulsion [6,17]. As the size of the molecule increases, δ decreases, reflecting the ability of the two final state holes to stay apart from each other in the delocalized molecular orbitals. Note also that for similar sized molecules, the δ 's for the alkenes are smaller than for the alkanes. This may reflect the increased screening due to the π electrons.

4.2 The resonant satellites

Resonant satellites are present in the polyethylene line shape [9], but not in diamond or graphite [7,8]. This is because polyethylene has an excitonic level as seen by x-ray absorption (XAS) [24] and electron energy loss (EELS) [25] data. In diamond and graphite, no such excitonic level exists so that the resonantly excited electron does not remain as a spectator or participator in the Auger decay [7,8,26]. In small molecules, the resonantly excited electron cannot escape, so that under electron excitation, resonant satellites are expected. Similar resonant satellites have in fact been observed in XES spectra (e.g. see Fig. 2b) [27,28].

Table 2 summarizes the resonant satellites as characterized by their relative intensities and energy shifts, $\delta_{K\alpha-V}$ and $\delta_{K\alpha-VV\alpha}$. Note that the $K\alpha$ -V and $K\alpha$ -VV intensities are all around 6-13% and the $K\alpha$ -V less than 3%. The intensities of the resonant satellites depend on the electron excitation energy and the secondary cascade process, so that their absolute intensities are not very interesting. It should be pointed out, however, that by utilizing synchrotron radiation tuned to the exact resonant energy, one could obtain

experimentally just the resonant contributions [29]. This process has been called de-excitation electron spectroscopy (DES), and has been reported for both gas phase and chemisorbed CO, where the $2\pi^*$ level is resonantly populated [29].

Although their individual intensities are not of interest, the ratio of intensities, $I(ke-v)/I(ke-vve)$, indicates something about the character of the excitonic level. The atomic Auger matrix elements per electron are essentially the same, for the ss, sp and pp contributions in kvv spectra [7]. Therefore, we can estimate what the ratio of intensities should be, based purely on the ratio of local electron densities, assuming a completely localized excitonic level. With an initial state charge distribution of $\sigma_s\sigma_p^2$ or $\sigma_s\sigma_p^2\pi_e$, $I(ke-v)/I(ke-vve)$ should be 0.5, compared with ≈ 0.14 for the alkenes and ≈ 0.25 for polyethylene [9], found experimentally. This suggests that although the excitonic level may be localized in time, it must be of a more diffuse nature spatially. The factor of two or more reduction from that expected theoretically suggests that the core exciton spends only part of its time on the methyl group with the core hole, the other part of the time presumably on neighboring carbon atoms or methyl groups.

The much smaller $I(ke-v)/I(ke-vve)$ ratio for the alkenes (≈ 0.14) compared with polyethylene (≈ 0.25) arises because of the different nature of the excitonic orbitals [6]. In the alkenes, this orbital is the antibonding π orbital. Charge moves toward a core hole in a bonding orbital, but away from it in an antibonding orbital. Therefore, in ethylene or benzene, we would expect the excited electron to spend more time on the carbon atom opposite or away from the core hole than on the carbon atom with the core hole, in agreement with experiment. In contrast, the σ^* excitonic level in polyethylene is antibonding in character within the immediate methyl group, but bonding in character between methyl groups (i.e. it is antibonding w/r to C-H but

bonding w/r to C-C). Therefore charge moves toward the methyl group with the core hole. However, the result above suggests that the excited electron still spends nearly half of its time on nearest neighbor methyl groups.

Table 2 also summarizes the required shifts, $\delta_{K\alpha-v}$ and $\delta_{K\alpha-vv}$ for the resonant satellites. $\delta_{K\alpha-v}$ should be equal to the binding energy of the excitonic electron. We compare $\delta_{K\alpha-v}$ with the binding energies obtained from EELS data [30] in Table 2. Good agreement between these two results are obtained.

The shifts $\delta_{K\alpha-vv}$ vary over a large range, although these shifts are much larger for the alkanes than for the alkenes. This reflects the greater screening of the final state holes by an electron in a π^* orbital compared with that in a diffuse Rydberg orbital. The difference in shifts,

$$\Delta\delta = \delta_{K\alpha-vv} - \delta_{K\alpha-v} = 2U_{vv} - U_{cc} \quad (6)$$

should directly reflect the nature of the core, U_{cc} , and valence, U_{vv} , polarization energies [6,9]. These are tabulated in Table 2. We see that $\Delta\delta$ is generally about 5 eV for the alkanes and 8 eV for the alkenes.

4.3 The shakeoff satellites

We note that the relative intensities of the $kv-vvv$ satellites for the 6 molecules listed in Table 2 are essentially all around 20% to within experimental error. This is in contrast to graphite [7] and diamond [8], which indicated no initial state shake satellites. The absence of such satellites in graphite and diamond arises because the shake hole in the initial state of these covalently bonded solids does not stay localized near the core hole for a time sufficient to "witness" the Auger decay. We have shown elsewhere [9] that in the presence of a core hole, the occupied valence band DOS of diamond indeed does not exhibit any bound states. On the other hand, the DOS for polyethylene in the presence of a core hole does exhibit narrow peaks indicative of bound-like states, consistent with the initial state shake/Auger

satellite observed [9].

Methane is isoelectronic with the neon atom. The shakeoff probability for neon has been both measured and calculated to be around 21% [31,32], in excellent agreement with that found for all of the carbon systems in this work. This agreement provides further empirical evidence for the validity of the methyl sub-unit orbital picture in these carbon systems.

Column 3 of Table 2 shows that the most appropriate ΔU for the kv-vvv satellite is the same as that for the kvv line shape in the alkanes, but twice that for the kvv line shape in the alkenes. As mentioned above, this means that for the alkenes, the shake hole is localized primarily on the methyl group with the core hole (case 1), but in the alkenes the shake hole is more delocalized onto some sub-cluster of the alkane chain (case 2). We attribute this different behavior to the different polarization lengths in the alkanes and the alkenes. In the alkenes, the π electrons screen the core hole, reducing the polarization potential which neighboring methyl groups experience. Thus the neighboring methyl groups remain in the band and the shake hole stays localized on the primary methyl group containing the core hole. In the alkanes, the core hole potential "pulls down" not only the primary methyl group, but the neighboring methyl groups are partially "pulled down" as well, enabling the shake hole to partially delocalize over the neighboring methyl groups [6].

Finally, in columns 4 and 5 of Table 2, we consider the optimal shifts, δ_{kv-vvv} , of the theoretical kv-vvv satellite. Column 4 indicates how the kv-vvv satellite was generated. For the alkanes, the kv-vvv line shape has exactly the same shape as the kvv line shape and it is simply shifted down by an amount $\delta_{kv-vvv} - \delta_{kvv}$. For the alkenes, the δ_{kv-vvv} shifts are generated by doubling the δ_{kvv} shifts, consistent with the doubling of the ΔU 's. For benzene, an additional shift of 4 eV was added to provide optimal agreement

with experiment [6]. Column 5 gives the total shift relative to the one-electron picture for the major CH-CH bonding contribution. Column 5 reveals no systematic change in $\delta(\text{CH-CH})$, indeed to within experimental error, it is essentially constant. This is in contrast to the δ_{kv} tabulated in Table 1, where we see that as the molecules get larger, the δ_{kv} decrease for both the alkanes and alkenes. We conclude that in the three-hole final state of the kv-vvv process, the three holes are consistently localized on some sub-cluster of the molecule (i.e., a methyl group), whereas in the kvv process, the two-holes are delocalized throughout the molecule [33,34]. Again we see, that the larger the repulsive forces, the more localized the final state holes, consistent with the Cini theory [15].

Table 2 shows that the empirically determined intensity for the k-vvv satellite is quite constant around 17%. This intensity was determined by integrating the area under the Bethe expression [6] from E_u down to $E_u + 50$ eV. This includes most of the final state shake satellite although some intensity exist beyond this region. This could easily introduce an error of 3%, so that to within experimental error, the initial and final state satellite intensities are similar, as expected.

5. Summary

We summarize the results as follows:

- 1) The normal kvv line shape accounts for only about half of the total experimental intensity for the gas phase molecules. This is in contrast to polyethylene where it accounts for 70% [9] and in diamond and graphite where it accounts for 100% [7,8].
- 2) Significant parts of the experimental line shape can be attributed to 3 different satellite contributions; namely resonant excitation, initial-state-shake, and final-state shake satellites (i.e. via ke-vve, kv-vvv, and k-vvv processes).
- 3) In contrast to that reported previously [33,34], the normal kvv Auger

line shapes reflect delocalized holes, but correlation effects are evident. In contrast, the 3-hole final state of the kv - vvv process reflects holes localized primarily on a single methyl group.

4) The ΔU 's of the kvv line shape for the gas phase molecules and the solids are similar, indicating long range screening effects are not important. On the other hand, the kvv and kv - vvv line shapes reveal that π electron screening within the alkenes is important.

We note here that some controversy exist over the third conclusion above. Previously Rye and coworkers [33] concluded that even the normal kvv lineshapes for the hydrocarbons reflect localized holes. This conclusion was based on the qualitative energy alignment of the principal peak in the Auger lineshapes for the alkane series, methane to hexane [33], and even for polyethylene [23]. More recently Rye et al [34] found that even the line shape for ethylene/Ni at 80 K indicated a ΔU only slightly smaller than that for ethylene gas, in sharp contrast to that indicated above.

Much of the controversy arises because of uncertainty in the experimental absolute energy scales. For example, the two published line shapes for polyethylene [23,12], and for ethylene/Ni [20,34], have energy scales differing by about 5 eV. In both cases we used [9,10] the data which indicate the smallest ΔU and δ . This choice is based on consistency with other published data (i.e. where the energy scale has been more precisely determined), and with our theoretical approach which strongly couples the energy scale with the spectral line shape. Thus, for example, to increase the binding energy of the theoretical kvv line shape for polyethylene would require the line shape to become narrower and sharper (due to the nature of the Cini distortion), but this is not indicated by the experimental data. Further, the theoretical resonant contributions, where large hole-hole repulsions certainly do not exist, are not consistent with that data [23,34]

which is shifted to higher two-hole binding energy. We therefore believe that our third conclusion above is correct.

Finally, we point out a significant difference in character between the gas phase and chemisorbed hydrocarbon Auger line shapes [10]. In the gas phase, the C-C and C-H bonds are all similar in nature, so that delocalized molecular orbitals are formed. However, the Auger line shape reflects only the self-fold of the DOS, which obscures all but the gross features of these DOS. Thus, the comparable alkanes and alkenes have very similar DOS self-folds (e.g. see Fig. 1). The experimental line shapes reflect significant differences however. We have shown that this arises because of the different correlation effects in the $\sigma\sigma$ vs. the $\pi\pi$ contributions (i.e. ΔU is around 2 eV in the $\sigma\sigma$ and 0 in the $\pi\pi$). But, on the surface, we believe that all hole-hole correlation effects are effectively removed because of the charge transfer from the metal, so that the experimental line shapes now do reflect primarily the DOS self-fold. But now the bonds are not all similar, since the C-H and C-C bonds are very different in character from the C-M (metal substrate) bonds. In this case some molecular orbitals (MO's) are localized primarily on the molecular adsorbate, and some on the C-M adsorbate-substrate bond. Thus the experimental line shape for the chemisorbed systems has regions at higher two-hole binding energy which reflect the intramolecular MO's (the VV component) and those at lower binding energy which reflect the C-M MO's (the $V\pi^*$ and $\pi^*\pi^*$ components).

It is clear from this work that chemical effects in the Auger spectra arise primarily from the complex many-body effects (i.e. hole-hole correlation and screening), not from the simple one-electron DOS self-folds. This makes it a challenge to extract the chemical bonding information. Although some controversy still exists, much progress has been made over the last five years toward routinely meeting this challenge.

Table 1 Summary of ΔU and δ parameters obtained empirically for the theoretical kvv line shape [6-10].

Molecule	ΔU (eV)			δ^a (eV)		
	<u>CH-CH</u>	<u>CH-CC</u>	<u>CC-CC</u>	<u>CH-CH</u>	<u>CH-CC</u>	<u>CC-CC</u>
Alkanes						
Methane	0			12		
Ethane	1	1	0	12	10	10
Cyclohexane	3	3	1.25	9	9	9
Polyethylene	3	3	1.25	0	0	0
Diamond			2.			0
Alkenes	<u>$\sigma\sigma$</u>	<u>$\sigma\pi$</u>	<u>$\pi\pi$</u>	<u>$\sigma\sigma$</u>	<u>$\sigma\pi$</u>	<u>$\pi\pi$</u>
Ethylene	2	1	0	9	11	11
Benzene	2	1	0	8	6	6
Graphite	2	1	0	0	0	0

*A positive δ indicates a shift to higher two-hole binding energy.

Table 2 Summary of satellite characteristics [6-10]*

<u>ke-v</u>	<u>Rel. Int (%)</u>	<u>ΔU (eV)</u>	<u>δ^b (eV)</u>	<u>$E_s + U_{ss}$ (eV)</u>
Ethylene	2.	0	7.	6.3
Benzene	1.	0	5.	5.1
Polyethylene	3.		3.	2.9
Ethylene/Ni ($V\pi^$ comp)	27	0	0	-
<u>ke-vve</u>				<u>$\Delta\delta$</u>
Methane	12.	0	7.	5.
Ethane	12.	0	8	4
Cyclohexane	8.	0	4.	5.
Polyethylene	11.	0	-5.	5.
Ethylene	13.	0	3.	7.
Benzene	6.	0	-1.	8.
*Ethylene/Ni (VV comp)	45	0	0	-
<u>kv-vvv</u>				<u>$\delta_{(cs-cq)}$ (eV)</u>
Methane	20.	0	$\delta_{kv}+5$	17
Ethane	21.	ΔU_{kv}	$\delta_{kv}+5$	17
Cyclohexane	19.	ΔU_{kv}	$\delta_{kv}+11$	20
Polyethylene	17.-21.	ΔU_{kv}	18	18
Ethylene	20.	$2\Delta U_{kv}$	$2\delta_{kv}$	18
Benzene	21.	$2\Delta U_{kv}$	$2\delta_{kv}+4$	20
Ethylene/Ni (VV & $V\pi^$)	20	ΔU^c	$\delta_{kv}+5^c$	14
<u>k-vvv</u>	<u>Rel. Int (%)</u>	<u>E_{12} (eV)</u>	<u>kvv Int. (%)</u>	
Methane	17.	53	53.	
Ethane	15.	50	49.	
Cyclohexane	19.	53	50.	
Polyethylene	0		70.	
Ethylene	15.	50	54.	
Benzene	16.	50	54.	

*The characteristics of the π^*V and VV components of the primary kvv term for ethylene/Ni are also indicated because these resemble the satellite line shapes for ethylene gas.

^bA positive δ indicates a shift to higher two-hole binding energy.

^cThe ΔU and δ indicated here are that for gas phase ethylene.

References

1. "Standard Guide for Identifying Chemical Effects and Matrix Effects in Auger Electron Spectroscopy, in Annual Book of ASTM Standards, (American Society for Testing and Materials, Philadelphia, PA, 1984), p.1.
2. D.E. Ramaker, J.S. Murday, and N.H. Turner, J. Electron. Spectrosc. Related. Phenom. 17, 45 (1979).
3. J.E. Houston, in Methods of Surface Characterization, edited by C.J. Powell, T.E. Madey, J.T. Yates, A.W. Czanderna, and D.M. Hercules, (Plenum, New York, 1983), Vol. 1.
4. D.E. Ramaker, *Appl. Surf. Sci.* 21, 243 (1985).
5. See references 1 to 20 in ref. 4 above.
6. F.L. Hutson and D.E. Ramaker, J. Chem Phys. 87, 6824 (1987).
7. J.E. Houston, J.W. Rogers, R.R. Rye, F.L. Hutson, and D.E. Ramaker, *Phys. Rev. B* 34, (1986).
8. D.E. Ramaker and F.L. Hutson, *Solid State Commun.* 63, 335 (1987).
9. F.L. Hutson and D.E. Ramaker, *Phys. Rev. B* 35, 9799 (1987).
10. F.L. Hutson and D.E. Ramaker, submitted to *Phys. Rev. B*.
11. D.E. Ramaker, in "Chemistry and Physics of Solid Surfaces IV", ed. by R. Vanselow and R. Howe (Springer, Berlin, 1982) p. 19.
12. M. Dayan and S.V. Pepper, *Surf. Sci.* 138, 549 (1984); S.V. Pepper, *Appl. Phys. Lett.* 38, 345 (1981).
13. K. Siegbahn et al. "ESCA Applied to Free Molecules" (North Holland Publ. Co. New York, 1969), p. 103.
14. J.E. Houston and R.R. Rye, J. Chem. Phys. 74, 71 (1981).
15. M. Cini, *Solid. State Commun.* 20, 655 (1976); *Phys. Rev. B* 17, 2788 (1978); G.A. Sawatzky, *Phys. Rev. Letters* 39, 504 (1977).
16. D.E. Ramaker, *Phys. Rev. B* 21, 4608 (1980).
17. B.I. Dunlap, F.L. Hutson, and D.E. Ramaker, *J. Vac. Sci. Technol.* 18, 556 (1981).

18. W.L. Jorgensen and L. Salem, "The Organic Chemists Book of Orbitals" (Academic, New York, 1973).
19. D.E. Ramaker, Phys. Rev. B25, 7341 (1982).
20. B. Koel, private communication, to be published.
21. R.R. Rye, D.R. Jennison, and J.E. Houston, J. Chem. Phys. 73, 4867 (1980); D.R. Jennison, Chem. Phys. Letters 69, 435 (1980).
22. P.G. Lurie and J.M. Wilson, Surf. Sci. 65, 453 (1977).
23. J.A. Kelber, R.R. Rye, G.C. Nelson, and J.E. Houston, Surf.Sci. 116, 148 (1982).
24. K. Seki et al., J. Chem. Phys. 66, 3644 (1977); M. Fujihira and H. Inokuchi, Chem. Phys. Letters 17, 554 (1972).
25. J.J. Ritsko, J. Chem. Phys. 70, 5345 (1979).
26. J.F. Morar et al., Phys. Rev. Letters 54, 1960 (1985).
27. R.A. Mattson and R.C. Ehlert, J. Chem. Phys. 48, 5465 (1968).
28. J. Nordgren, L. Selander, L. Pettersson, R. Brammer, M. Backstrom, and C. Nordling, Phys. Scripta 27, 169 (1983).
29. C.T. Chen, R.A. DiDio, W.K. Ford, E.W. Plummer, and W. Eberhardt, Phys. Rev. B32, 8434 (1985).
30. A.P. Hitchcock and C.E. Brion, J. Electron. Spectrosc. Related Phenom. 10, 317 (1977).
31. T.A. Carlson, Radiat. Res. 64, 53 (1975); T.A. Carlson, C.W. Nestor, Jr., T.C. Tucker, and F.B. Malik, Phys. Rev. 169, 27 (1968).
32. D.E. Ramaker and J.S. Murday, J. Vac. Sci. Technol. 16, 510 (1979).
33. R.R. Rye, T.E. Madey, J.E. Houston, and P.H. Holloway, J. Chem. Phys. 69, 1504 (1978); Ind. Eng. Chem. Prod. Res. Dev. 18, 2 (1979); J. Chem. Phys. 73, 4867 (1980).
34. R.R. Rye, C.M. Greenlief, D.W. Goodman, E.L. Hardegree, and J.M. White, Surf. Sci. xxx, xxx (1988).

Figure Captions

- Fig. 1** Comparison of the experimental C KVV Auger line shapes (solid line) obtained from the literature for diamond [12], graphite [7], benzene [13], cyclohexane [14], and polyethylene [12] with the self-fold of the DOS (dotted line) obtained as described in the text.
- Fig. 2** Summary of the various processes giving rise to the total Auger line shape. Core, VB and CB indicate the core level, valence band (or filled orbitals), and conduction band (or empty orbitals) respectively. Spec. (spectator) and part. (participant) indicate the subsequent fate of the resonantly excited electron during the Auger process. I.s and f.s. indicate initial-state and final-state and refer to the state in which the shakeoff event occurs relative to the Auger decay. N*N and N refer to the approximate line shape, i.e. either a DOS self-fold, or just the DOS, with the relative size of ΔU in the Cini expression (eq. 4) indicated. The resonant satellites occur only under electron excitation.
- Fig. 3** a) Comparison of the C KVV experimental [21] and theoretical [6] Auger line shapes for ethylene gas. The various contributions (kvv, kv-vvv, k-vvv, ke-v, ke-evv) were obtained as described in the text.
b) Comparison of the experimental [20] and theoretical [10] Auger line shapes for ethylene chemisorbed on Ni(100) at 100 K (π -bonded ethylene). The three components (VV, $V\pi^*$, $\pi^*\pi^*$) line shapes were obtained as described in the text. The relative intensities were obtained by least squares fit to the experimental data.
- Fig. 4** a) Comparison of the experimental C KVV line shape for benzene [13] with the total theoretical line shape [6] obtained as described in the text.
b) The total theoretical line shape and each of the components as

indicated

c) Comparison of the satellite components with the difference spectrum (experimental - theoretical kvv component).

Fig. 5

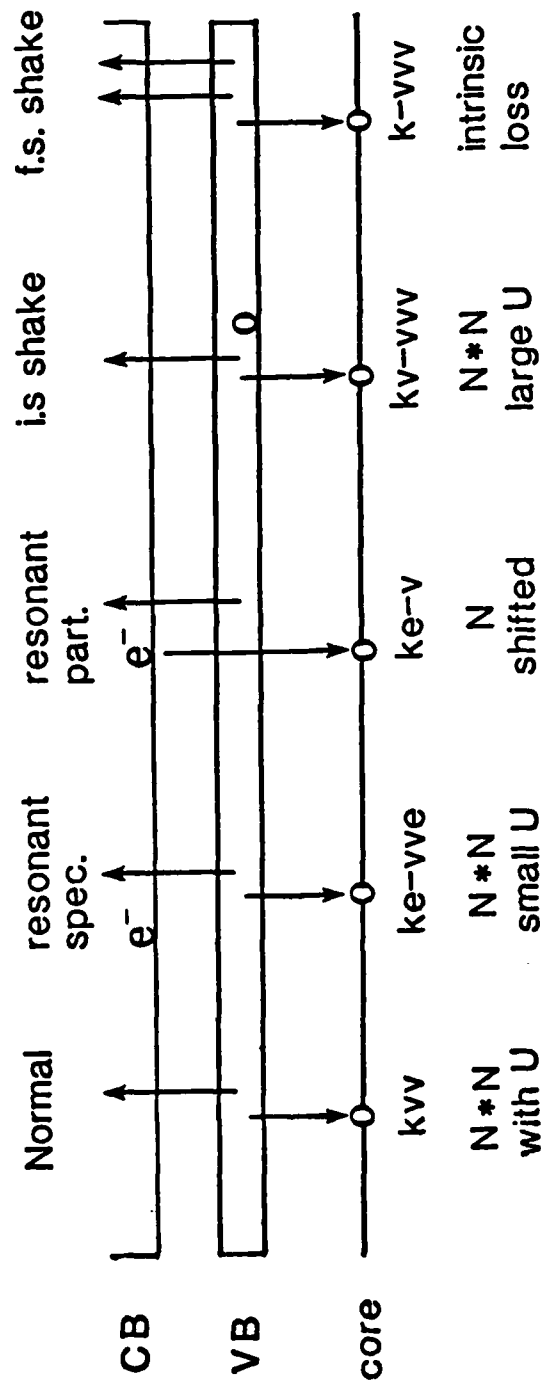
a) Comparison of the experimental Auger line shape for polyethylene (from Kelber et al [23] and Dayan and Pepper [12]) with the theoretical total line shape [9] determined as described in the text. The components in order of increasing energy are kv-vvv, kvv, ke-vve, and ke-v.

b) Comparison of the difference spectra (Dayan's experimental spectrum minus the theoretical kvv component) with the sum of the satellite components.

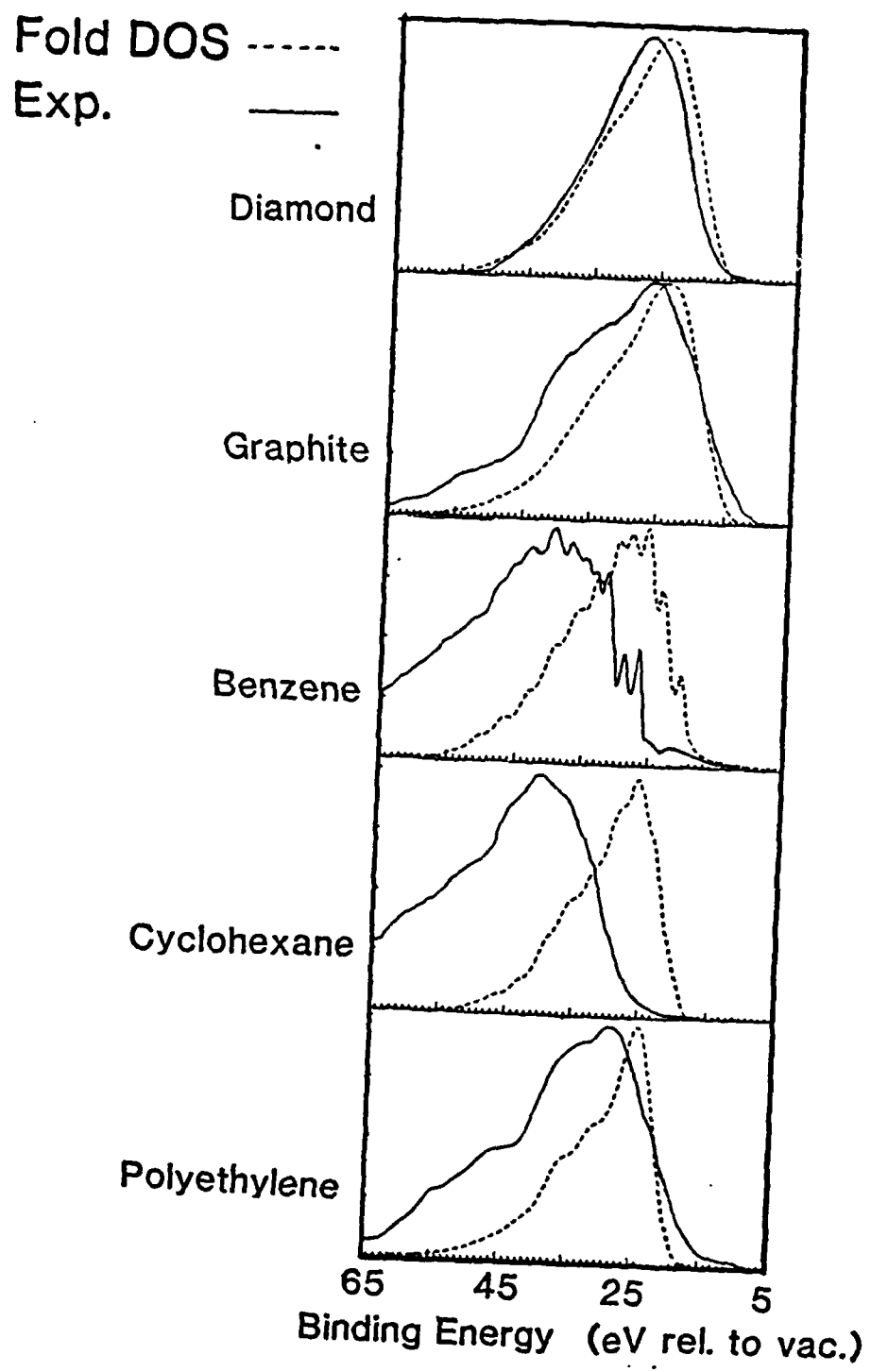
Fig. 6.

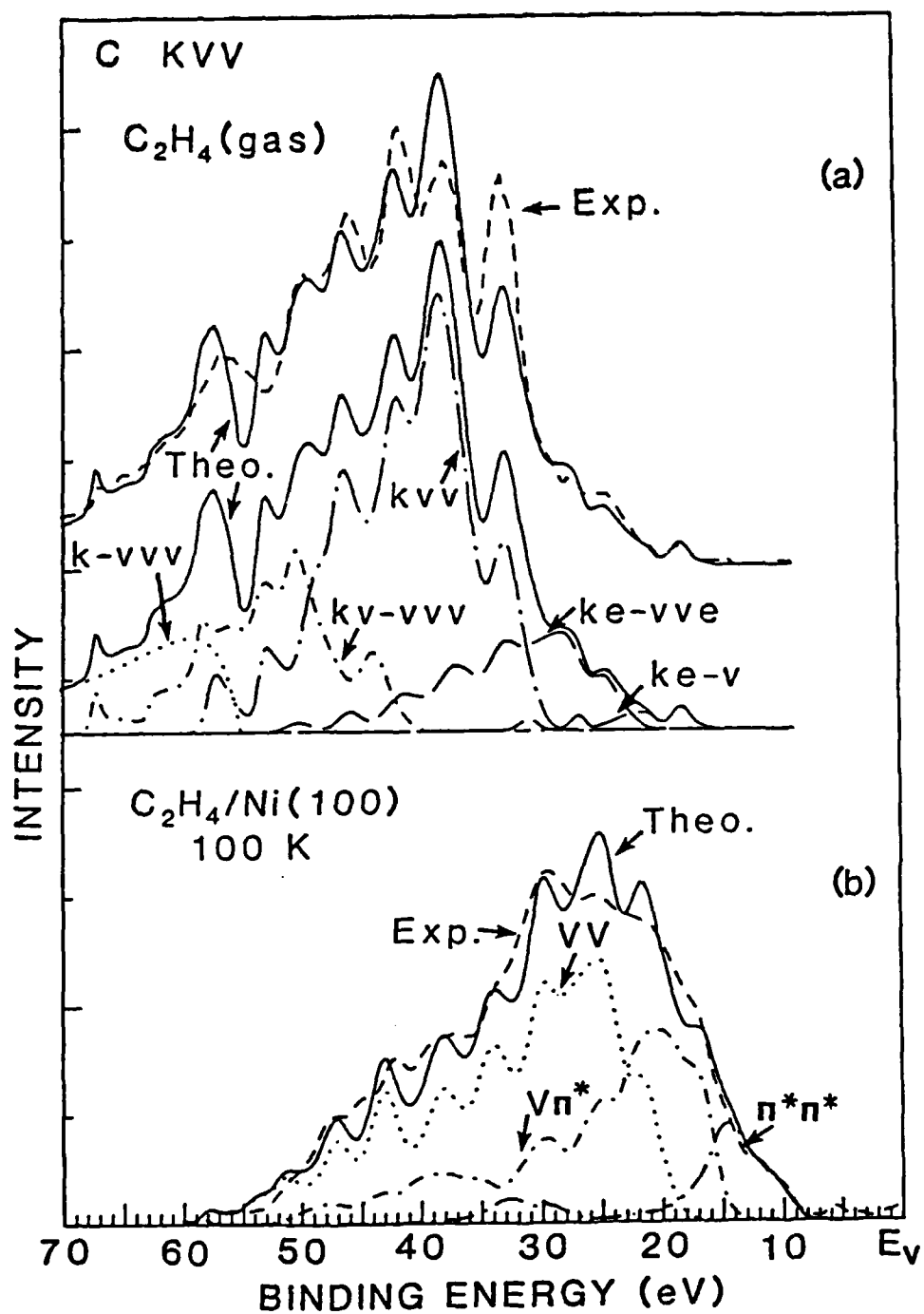
a) Comparison of the C KVV Auger derivatives ($dN(E)/dE$ and $dA(E)/dE$) for the H terminated [12] and clean [22] reconstructed (111) - (2 x 1) surfaces of diamond. The $dA(E)/dE$ lineshapes result after the background subtraction and deconvolution procedures, while $dN(E)/dE$ is the as measured data. The H-terminated line shape is more representative of the bulk since C-H bonds are more similar to bulk C-C bonds than the π bonds existing in the surface reconstruction.

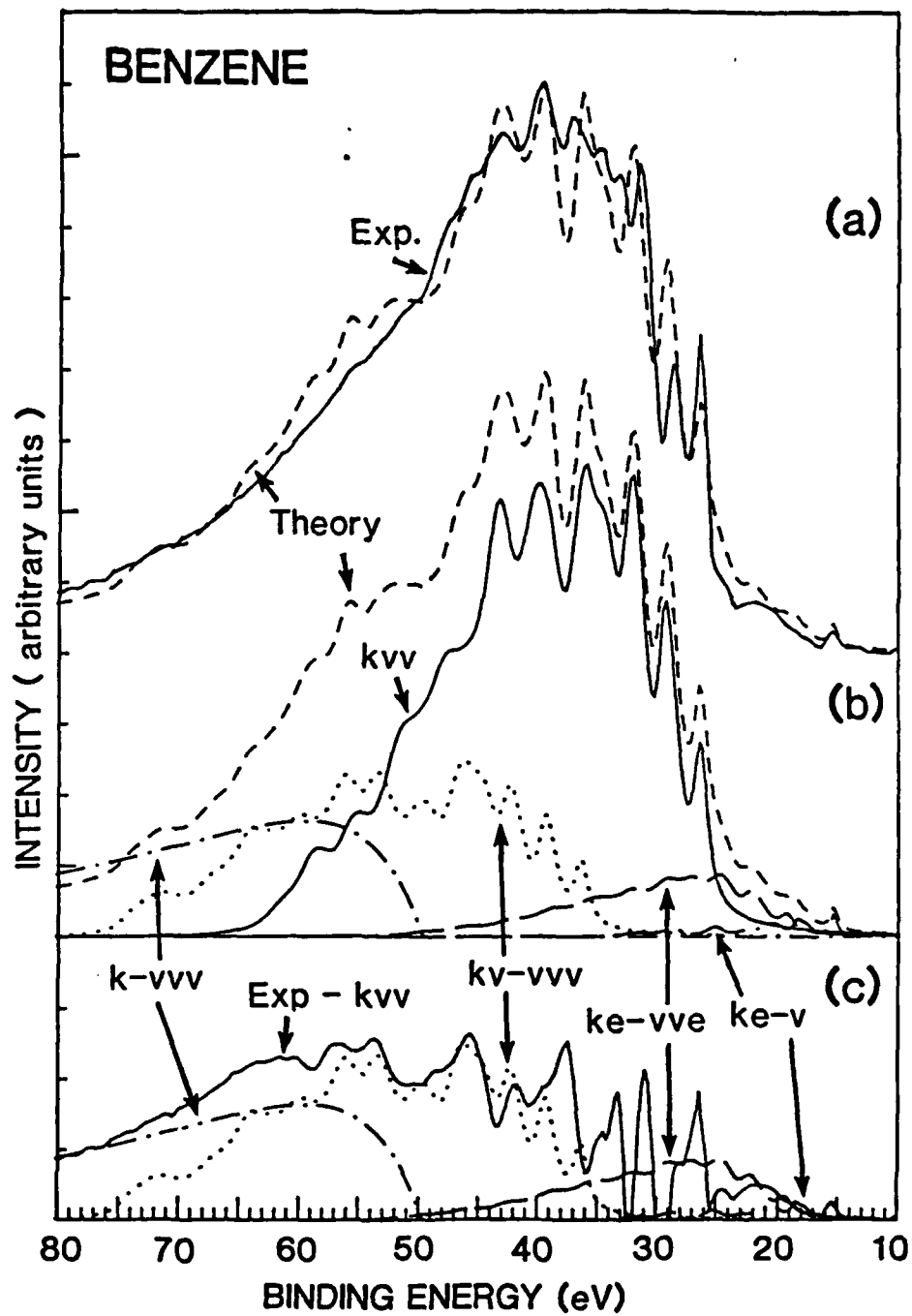
b) Comparison of the $A(E)$ lineshapes determined from above. Also shown is a comparison of the H terminated line shape with the theoretical kvv line shape [8] determined as described in the text. The s^*s , s^*p , and p^*p components have maxima at 248, 258, and 268 eV, respectively.

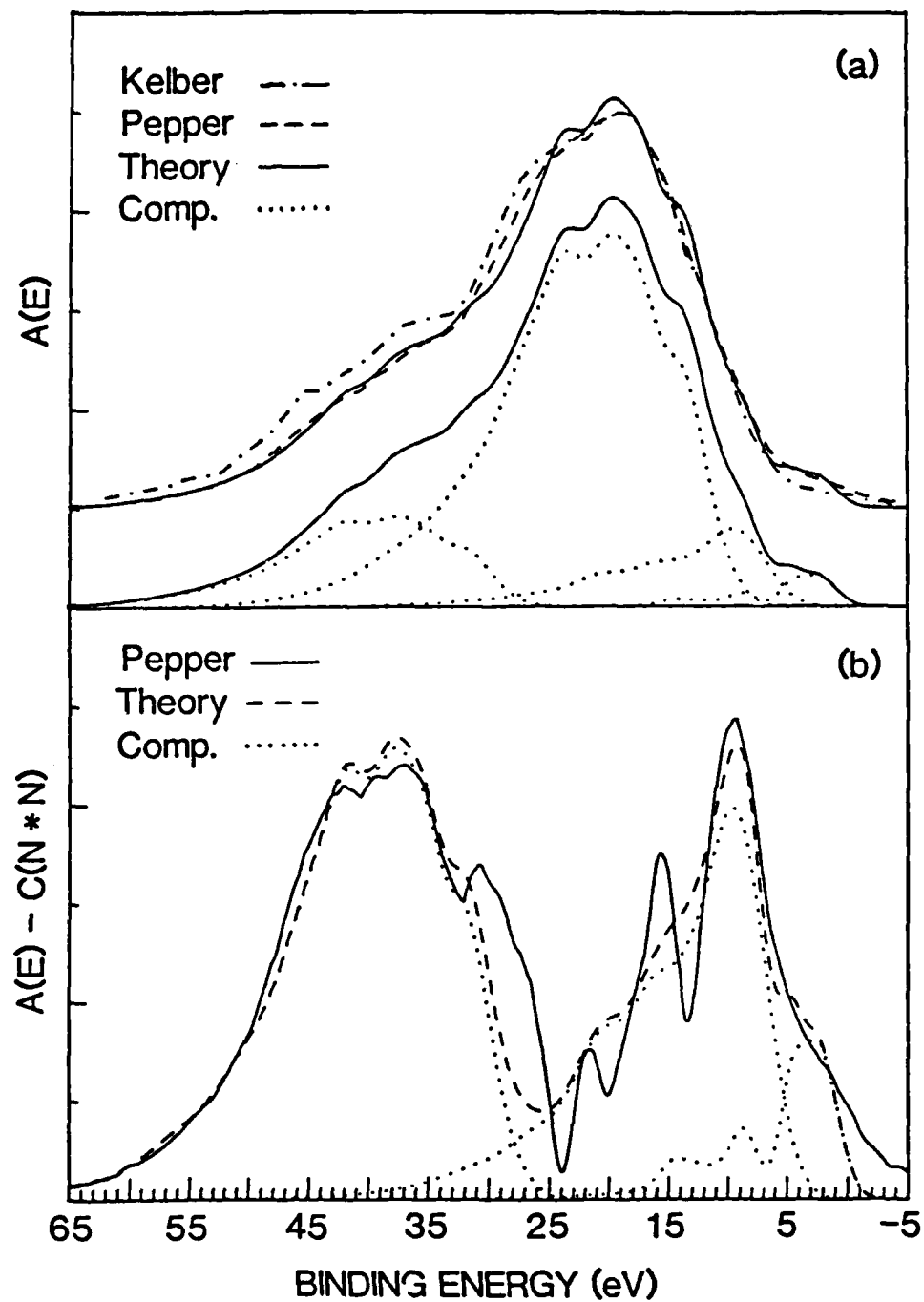


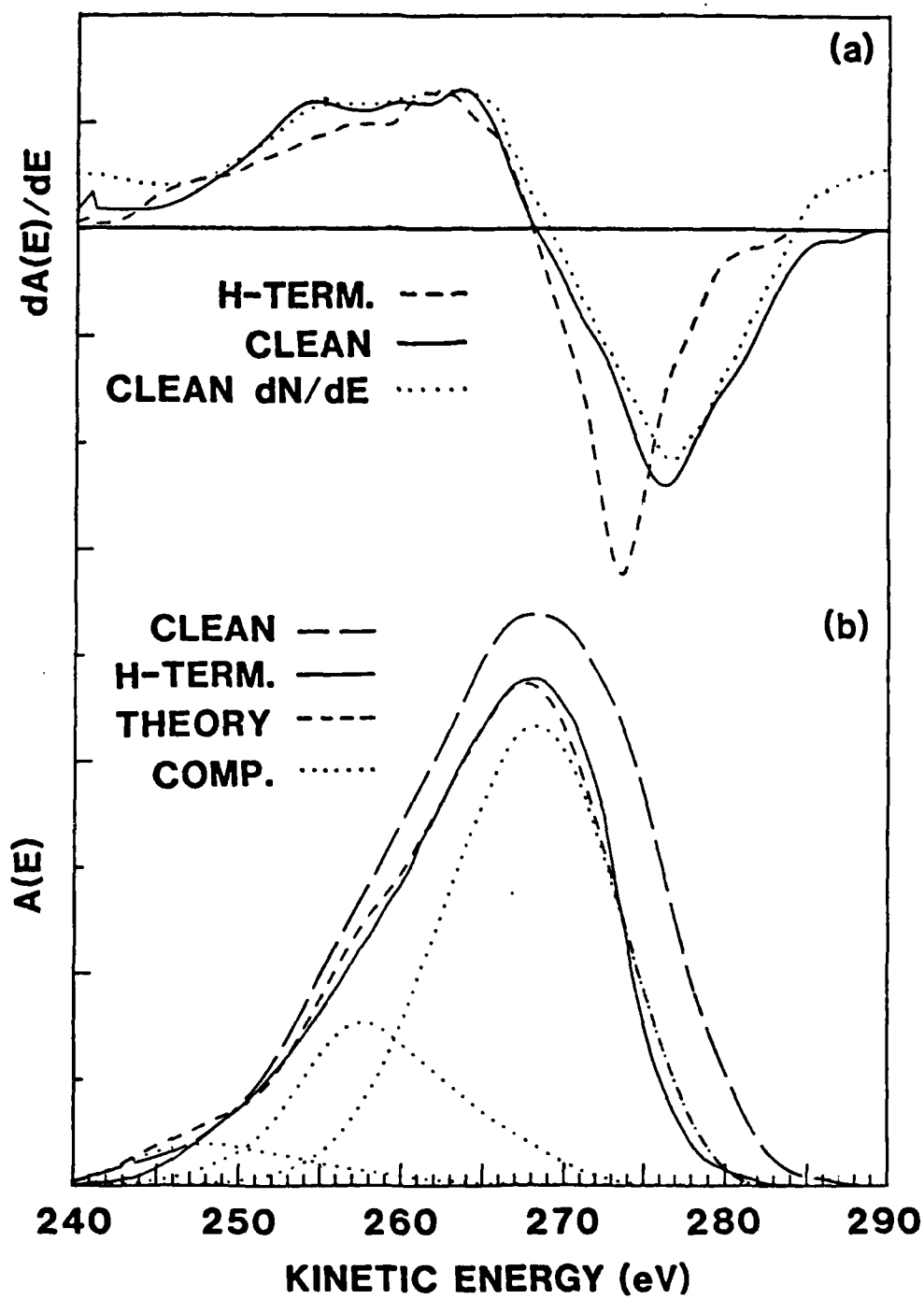
e^- excitation only











DL/1113/87/2

TECHNICAL REPORT DISTRIBUTION LIST, GEN

	<u>No. Copies</u>		<u>No. Copies</u>
Office of Naval Research Attn: Code 1113 800 N. Quincy Street Arlington, Virginia 22217-5000	2	Dr. David Young Code 334 NORDA NSTL, Mississippi 39529	1
Dr. Bernard Duda Naval Weapons Support Center Code 50C Crane, Indiana 47522-5050	1	Naval Weapons Center Attn: Dr. Ron Atkins Chemistry Division China Lake, California 93555	1
Naval Civil Engineering Laboratory Attn: Dr. R. W. Drisko, Code L52 Port Hueneme, California 93401	1	Scientific Advisor Commandant of the Marine Corps Code RD-1 Washington, D.C. 20380	1
Defense Technical Information Center Building 5, Cameron Station Alexandria, Virginia 22314	12 high quality	U.S. Army Research Office Attn: CRD-AA-IP P.O. Box 12211 Research Triangle Park, NC 27709	1
DTNSRDC Attn: Dr. H. Singerman Applied Chemistry Division Annapolis, Maryland 21401	1	Mr. John Boyle Materials Branch Naval Ship Engineering Center Philadelphia, Pennsylvania 19112	1
Dr. William Tolles Superintendent Chemistry Division, Code 6100 Naval Research Laboratory Washington, D.C. 20375-5000	1	Naval Ocean Systems Center Attn: Dr. S. Yamamoto Marine Sciences Division San Diego, California 91232	1

ABSTRACTS DISTRIBUTION LIST, 056/625/629

Dr. F. Carter
Code 6170
Naval Research Laboratory
Washington, D.C. 20375-5000

Dr. Richard Colton
Code 6170
Naval Research Laboratory
Washington, D.C. 20375-5000

Dr. Dan Pierce
National Bureau of Standards
Optical Physics Division
Washington, D.C. 20234

Dr. R. G. Wallis
Department of Physics
University of California
Irvine, California 92664

Dr. D. Bamaker
Chemistry Department
George Washington University
Washington, D.C. 20052

Dr. J. C. Hemminger
Chemistry Department
University of California
Irvine, California 92717

Dr. T. F. George
Chemistry Department
University of Rochester
Rochester, New York 14627

Dr. G. Rubloff
IBM
Thomas J. Watson Research Center
P.O. Box 218
Yorktown Heights, New York 10598

Dr. J. Baldeschwieler
Department of Chemistry and
Chemical Engineering
California Institute of Technology
Pasadena, California 91125

Dr. Galen D. Stucky
Chemistry Department
University of California
Santa Barbara, CA 93106

Dr. A. Steckl
Department of Electrical and
Systems Engineering
Rensselaer Polytechnic Institute
Troy, New York 12181

Dr. John T. Yates
Department of Chemistry
University of Pittsburgh
Pittsburgh, Pennsylvania 15260

Dr. R. Stanley Williams
Department of Chemistry
University of California
Los Angeles, California 90024

Dr. R. P. Messmer
Materials Characterization Lab.
General Electric Company
Schenectady, New York 22217

Dr. J. T. Keiser
Department of Chemistry
University of Richmond
Richmond, Virginia 23173

Dr. R. W. Plummer
Department of Physics
University of Pennsylvania
Philadelphia, Pennsylvania 19104

Dr. E. Yeager
Department of Chemistry
Case Western Reserve University
Cleveland, Ohio 44106

Dr. N. Winograd
Department of Chemistry
Pennsylvania State University
University Park, Pennsylvania 16802

Dr. Roald Hoffmann
Department of Chemistry
Cornell University
Ithaca, New York 14853

Dr. Robert L. Whetten
Department of Chemistry
University of California
Los Angeles, CA 90024

Dr. Daniel M. Neumark
Department of Chemistry
University of California
Berkeley, CA 94720

Dr. G. H. Morrison
Department of Chemistry
Cornell University
Ithaca, New York 14853

ABSTRACTS DISTRIBUTION LIST, 056/625/629

Dr. J. E. Jensen
Hughes Research Laboratory
3011 Malibu Canyon Road -
Malibu, California 90265

Dr. J. H. Weaver
Department of Chemical Engineering
and Materials Science
University of Minnesota
Minneapolis, Minnesota 55455

Dr. A. Reisman
Microelectronics Center of North Carolina
Research Triangle Park, North Carolina
27709

Dr. M. Grunze
Laboratory for Surface Science
and Technology
University of Maine
Orono, Maine 04469

Dr. J. Butler
Naval Research Laboratory
Code 6115
Washington D.C. 20375-5000

Dr. L. Interante
Chemistry Department
Rensselaer Polytechnic Institute
Troy, New York 12181

Dr. Irvin Heard
Chemistry and Physics Department
Lincoln University
Lincoln University, Pennsylvania 19352

Dr. K. J. Klaubunde
Department of Chemistry
Kansas State University
Manhattan, Kansas 66506

Dr. C. B. Harris
Department of Chemistry
University of California
Berkeley, California 94720

Dr. R. Bruce King
Department of Chemistry
University of Georgia
Athens, Georgia 30602

Dr. R. Reeves
Chemistry Department
Rensselaer Polytechnic Institute
Troy, New York 12181

Dr. Steven M. George
Stanford University
Department of Chemistry
Stanford, CA 94305

Dr. Mark Johnson
Yale University
Department of Chemistry
New Haven, CT 06511-8118

Dr. W. Knauer
Hughes Research Laboratory
3011 Malibu Canyon Road
Malibu, California 90265

Dr. Theodore E. Madey
Surface Chemistry Section
Department of Commerce
National Bureau of Standards
Washington, D.C. 20234

Dr. J. E. Demuth
IBM Corporation
Thomas J. Watson Research Center
P.O. Box 218
Yorktown Heights, New York 10598

Dr. M. G. Lagally
Department of Metallurgical
and Mining Engineering
University of Wisconsin
Madison, Wisconsin 53706

Dr. R. P. Van Duyne
Chemistry Department
Northwestern University
Evanston, Illinois 60637

Dr. J. M. White
Department of Chemistry
University of Texas
Austin, Texas 78712

Dr. Richard J. Saykally
Department of Chemistry
University of California
Berkeley, California 94720

ABSTRACTS DISTRIBUTION LIST, 056/625/629

Dr. G. A. Somorjai
Department of Chemistry
University of California
Berkeley, California 94720

Dr. J. Murday
Naval Research Laboratory
Code 6170
Washington, D.C. 20375-5000

Dr. W. T. Peria
Electrical Engineering Department
University of Minnesota
Minneapolis, Minnesota 55455

Dr. Keith H. Johnson
Department of Metallurgy and
Materials Science
Massachusetts Institute of Technology
Cambridge, Massachusetts 02139

Dr. S. Sibener
Department of Chemistry
James Franck Institute
5640 Ellis Avenue
Chicago, Illinois 60637

Dr. Arold Green
Quantum Surface Dynamics Branch
Code 3817
Naval Weapons Center
China Lake, California 93555

Dr. A. Wold
Department of Chemistry
Brown University
Providence, Rhode Island 02912

Dr. S. L. Bernasek
Department of Chemistry
Princeton University
Princeton, New Jersey 08544

Dr. W. Kohn
Department of Physics
University of California, San Diego
La Jolla, California 92037

Dr. Stephen D. Kevan
Physics Department
University Of Oregon
Eugene, Oregon 97403

Dr. David M. Walba
Department of Chemistry
University of Colorado
Boulder, CO 80309-0215

Dr. L. Kesmodel
Department of Physics
Indiana University
Bloomington, Indiana 47403

Dr. K. C. Janda
University of Pittsburg
Chemistry Building
Pittsburg, PA 15260

Dr. E. A. Irene
Department of Chemistry
University of North Carolina
Chapel Hill, North Carolina 27514

Dr. Adam Heller
Bell Laboratories
Murray Hill, New Jersey 07974

Dr. Martin Fleischmann
Department of Chemistry
University of Southampton
Southampton SO9 5NH
UNITED KINGDOM

Dr. H. Tachikawa
Chemistry Department
Jackson State University
Jackson, Mississippi 39217

Dr. John W. Wilkins
Cornell University
Laboratory of Atomic and
Solid State Physics
Ithaca, New York 14853

Dr. Ronald Lee
R301
Naval Surface Weapons Center
White Oak
Silver Spring, Maryland 20910

Dr. Robert Gomer
Department of Chemistry
James Franck Institute
5640 Ellis Avenue
Chicago, Illinois 60637

Dr. Horia Metiu
Chemistry Department
University of California
Santa Barbara, California 93106

Dr. W. Goddard
Department of Chemistry and Chemical
Engineering
California Institute of Technology
Pasadena, California 91125